PEPTIDES 27 (2006) 575–582

available at www.sciencedirect.com

SCIENCE DIRECT®

journal homepage: www.elsevier.com/locate/peptides

Structural studies of *Drosophila* short neuropeptide F: Occurrence and receptor binding activity

Stephen F. Garczynski [a], *Mark R. Brown* [b], *Joe W. Crim* [a,*]

[a] *Department of Cellular Biology, University of Georgia, Athens, GA 30602, USA*
[b] *Department of Entomology, University of Georgia, Athens, GA 30602, USA*

ARTICLE INFO

Article history:
Received 7 April 2005
Accepted 20 June 2005
Published on line 5 December 2005

Keywords:
Insect
Drosophila
G protein-coupled receptor
Neuropeptide F
Neuropeptide Y

ABSTRACT

Among insects, short neuropeptide Fs (sNPF) have been implicated in regulation of reproduction and feeding behavior. For *Drosophila melanogaster*, the nucleotide sequence for the sNPF precursor protein encodes four distinctive candidate sNPFs. In the present study, all four peptides were identified by mass spectrometry in body extracts of *D. melanogaster*; some also were identified in hemolymph, suggesting potential neuroendocrine roles. Actions of sNPFs in *D. melanogaster* are mediated by the G protein-coupled receptor Drm-NPFR76F. Mammalian CHO-K1 cells were stably transfected with the Drm-NPFR76F receptor for membrane-based radioreceptor studies. Binding assays revealed that longer sNPF peptides comprised of nine or more amino acids were clearly more potent than shorter ones of eight or fewer amino acids. These findings extend understanding of the relationship between structure and function of sNPFs.

1. Introduction

For insects, short neuropeptide Fs (sNPF) were first identified in the Colorado potato beetle, *Leptinotarsa decemineata* [23]. Two peptides were obtained from extracts of brains and are now termed *Led*-sNPF1 (ARGPQLRLRFa) and *Led*-sNPF2 (APSLRLRFa). Subsequently, other insect sNPFs have been identified in desert locust (*Schistocerca gregaria*, see [6]), fruit fly (*Drosophila melanogaster* [25]), African malaria mosquito (*Anopheles gambiae* [21]), and yellow fever mosquito (*Aedes aegypti* [21]).

Emerging information suggests that sNPFs likely regulate physiological processes in insects. For example, administration of *Led*-sNPF1 to the migratory locust, *Locusta migratoria*, stimulates ovarian development [4,6], suggesting a role in reproduction. Recently, sNPFs have been implicated in the regulation of feeding behavior of *D. melanogaster* [13]. Manipulation of the *sNPF* gene containing the sNPF precursor affects food consumption in larvae and in adults. Gain-of-function *sNPF* mutants exhibit increased food intake, resulting in larger flies; loss-of-function *sNPF* mutants display reduced food intake [13]. These observations indicate that sNPFs have fundamental effects on the physiology of insects.

The actions of sNPFs apparently are exerted via G protein-coupled receptors. For *D. melanogaster*, the cognate receptor is Drm-NPFR76F, as shown by activation of heterologously expressed receptors [8,16,20]. Drm-NPFR76F is a member of a group of invertebrate receptors that are structurally related to the mammalian type 2 neuropeptide Y receptors [10]. As for vertebrates, these receptors have been implicated in regulation of feeding and related physiological processes (e.g., [27]).

The *sNPF* gene of *D. melanogaster* encodes a precursor protein containing four distinctive sNPF peptides [25]. Direct identification of specific sNPFs in tissues of *D. melanogaster* by proteomic approaches has met with only limited success [1,2,19]. Further, effects of candidate sNPFs on signaling events

* *Corresponding author*. Tel.: +1 706 542 3310; fax: +1 706 542 4271.
E-mail address: crim@cb.uga.edu (J.W. Crim).
0196-9781/$ – see front matter
doi:10.1016/j.peptides.2005.06.029

downstream from Drm-NPFR76F have varied depending on the cell system utilized for receptor expression [8,16,20].

The present study sought to clarify structure-function issues regarding sNPFs in *D. melanogaster*. First, we hypothesized that partial purification of extracts prior to analysis by mass spectrometry would increase the likelihood of detection of sNPF peptides. Accordingly, we used a radioimmunoassay for sNPF to guide purification of extracts of body and hemolymph. Second, we hypothesized that differences in structures among candidate sNPFs would be reflected in ability to bind to the Drm-NPFR76F receptor. Consequently, we stably transfected mammalian cells with the Drm-NPFR76F receptor and examined a panel of sNPF peptides by radioreceptor analysis. Both of these lines of investigation yielded new information about sNPFs of *D. melanogaster*.

2. Experimental procedures

2.1. DNA cloning

The EST clone, GH23382, encoding the CG7395 gene product (Drm-NPFR76F) was obtained from The Berkeley Drosophila Genome Project (BDGP). After the specific oligonucleotide primer (FWD 5′ CCG TAA AGA TGG CCA ACT TAA GCT GG 3′) and a pOT2 vector specific primer for the SP6 promoter (5′ GAT TTA GGT GAC ACT ATA G 3′), were added, receptor products were amplified by PCR from the EST clone with Taq-Titanium polymerase (1 U; total vol. 50 μl) and the following conditions; initial denaturation for 5 min at 95 °C, then amplification for 1 min at 95 °C, 1 min at 56 °C, 1 min at 72 °C for 30 cycles, followed by a 10 min 72 °C incubation. PCR products were separated on 1% agarose gels, and excised bands were purified using GenElute minus EtBr spin columns (Sigma). Purified PCR products were cloned into pCR®II-TOPO with TOP 10 *E. coli* competent cells (TOPO TA cloning® kit; Invitrogen, Carlsbad CA). For Drm-NPFR76F, 20 white colonies were picked, and plasmid DNA purified (QIAprep® spin miniprep kit, QIAGEN Inc., Valencia, CA). Potential Drm-NPFR76F clones were sequenced at Integrated Biotech Labs (IBT, University of Georgia, Athens, GA). The TA clones were digested with Eco RI and the resulting fragment (containing the ORF) was ligated into the mammalian expression vector pcDNA 3.1(+). The ligated products were transformed into TOP 10 *E. coli* competent cells and 20 colonies were picked, and plasmid DNA purified as above. Plasmids were analyzed for directionality and those in the proper orientation were used to transfect CHO-K1 cells. Transfection and selection were done as previously described [9]. Stable transfectants are herein referred to as Drm-NPFR76F cells.

2.2. Peptides and iodination

Sequences for sNPFs were deduced from the cloned cDNA or genomic predictions and synthesized (Table 1): Drm-sNPF1, 1D-Y^0, $2_{9–19}$ (86% pure; Quality Controlled Biochemicals Inc., Hopkinton, MA), 2 (80% pure; IBT), $1_{4–11}$, $2_{11–19}$, $2_{11–19}$R11A, 3, 4, Ang-sNPF1, 2, $2_{4–11}$, 3, 4, 5, Aea-sNPF2 (>80% pure; Dr. Kevin Clark, University of Georgia, Athens, GA), and Drm-NPF (see [3,9]). Peptide YY (PYY) was from Bachem Bioscience Inc. (King of Prussia, PA). Sequences encoding putative sNPFs in the mosquitoes, *Anopheles gambiae* and *Aedes aegypti*, were identified using TBlastN homology searches on sequences available through ENSEMBL (*A. gambiae*; http://www.ensembl.org/Anopheles_gambiae/) and TIGR (*A. aegypti*; http://www.tigr.org/tdb/e2k1/aabe/), and subsequently synthesized (Table 1).

Table 1 – Peptide sequences, abbreviations, and activities in radioreceptor assay

Abbreviation	Sequence	IC_{50} (nM)[a]
D. melanogaster[b] sNPF		
Drm-sNPF1	AQRSPSLRLRFa	**0.3**
Drm-sNPF1$_{4–11}$	SPSLRLRFa	9.0
Drm-sNPF2	WFGDVNQKPIRSPSLRLRFa	**0.3**
Drm-sNPF2$_{9–19}$	PIRSPSLRLRFa	**0.2**
Drm-sNPF2$_{11–19}$	RSPSLRLRFa	**0.4**
Drm-sNPF3	PMRLRWa	7.5
Drm-sNPF4	PQRLRWa	22.3
Analog		
Drm-sNPF2$_{11–19}$R11A	ASPSLRLRFa	12.7
A. gambiae[c]/ *A. aegypti*[d] sNPF		
Ang-sNPF1 (Aea-sNPF1)	AVRSPSLRLRFa	**0.2**
Ang-sNPF2 (Aea-sNPF4)	AIRAPQLRLRFa	**0.6**
Aea-sNPF2	SIRAPQLRLRFa	**1.0**
Ang-sNPF2$_{4–11}$ (Aea-sNPF2$_{4–11}$)	APQLRLRFa	13.7
Ang-sNPF3 (Aea-sNPF3)	APSQRLRWa	16.6
Ang-sNPF4	TIRAPQLRLRFa	**0.9**
Ang-sNPF5	APTQRLRWa	22.2
A. aegypti Head Peptide[e]		
Aea-HPI	pERPhPSLKTRFa	42.4
Aea-HPIII	pERPPSLKTRFa	n.a.[f]

[a] Values ≤1.0 nM shown in bold.
[b] Sequences from [25].
[c] Sequences from ENSEMBL transcript.
[d] Sequences from TIGR cDNA.
[e] Sequences from [14].
[f] n.a. indicates not active at 1 μM.

Drm-sNPF1D-Y^0, PYY and Drm-neuropeptide F (NPF) were iodinated by a lactoperoxidase—hydrogen peroxide method [5]. For each peptide, the radiolabeled mixture was loaded into a Beckman chromatography 421A/110B system HPLC and fractionated on a reverse phase C_8 column (Vydac, 300 Å, 4.6 × 150 mm); solvent A, water with 0.1% trifluoroacetic acid (TFA), and solvent B, 80% CH_3CN in solvent A (gradient program: 0–57% B, 10 min, 57–60% B, 50 min, 60–100% B, 10 min; 1 ml/min). ^{125}I-labeled peptides were detected with an in-line Beckman Model 170 radioisotope detector, and fractions containing the radiolabeled peptide were collected, with bovine serum albumin (BSA; Fraction V; Sigma) added to 1%. Fractions containing the radiolabeled peptide were diluted and counted on a Beckman Gamma 4000; final concentrations were determined based on specific activity (~2000 Ci/mmol) of ^{125}I in the product, which was free of unlabeled peptide and assumed to be monoiodinated.

2.3. Hemolymph collection and peptide extraction from whole bodies

Hemolymph was collected from 540 adult females. The thorax of each female was pierced and hemolymph was allowed to diffuse into *Aedes* saline (128 mM NaCl, 4.7 mM KCl, 1.9 mM $CaCl_2$) containing a protease inhibitor tablet (mini protean plus; Roche) for 15 min on ice. After diffusion, the saline containing hemolymph was pooled and frozen at −80 °C, then lyophilized.

For peptide extraction from whole insects, 1000 frozen adults were boiled in 20 ml of 3% acetic acid for 20 min. The acetic acid extract of the bodies was adjusted to 60 ml with 0.1% TFA and then applied to a Varian Mega Bond Elut C_{18} column (10 g sorbent mass) and then step eluted with 5% CH_3CN in 0.1% TFA, 60% CH_3CN in 0.1% TFA and then 100% CH_3CN. The material in the 60% CH_3CN in 0.1% TFA elution was lyophilized.

2.4. HPLC separation of hemolymph and whole body extracts

Initial separation of hemolymph, body extract, and synthetic Drm-sNPFs was achieved by reverse phase HPLC (Phenomenex Jupiter C_{18} column, 5 μm, 300 Å; 250 × 4.6 mm; solvent A, water with 0.1% TFA, and solvent B, 80% CH_3CN in solvent A; gradient program: 0–20% B, 5 min, 20–50% B, 40 min, 50–100% B, 10 min; 1 ml/min; monitored 206 nm). Aliquots were taken from all fractions obtained from the three HPLC separations and checked for immunoreactivity in the RIA (see below). Immunoreactive fractions from hemolymph and body extract were pooled separately and fractionated on a reverse phase C_8 column (Macrosphere 300, C8, 7 μm, 250 × 4.6 mm; solvent A, water with 0.01% heptafluorobutyric acid, and solvent B, 80% CH_3CN in solvent A; gradient program: 0–20% B, 5 min, 20–60% B, 40 min, 60–100% B, 10 min; 1 ml/min; monitored at 280 nm). Aliquots were taken from all fractions for the RIA. For the third step, immunoreactive fractions from hemolymph and the body extract were pooled separately and separated on the initial C_{18} column with the same conditions. Aliquots were taken from all fractions for the RIA. The mass weights of peptides in immunoreactive fractions were determined by MALDI (Chemical and Biological Sciences Mass Spectroscopy Facility, University of Georgia, Athens, GA).

2.5. Drm-sNPF radioimmunoassay

Pilot tests established that the rabbit antiserum 403C used in the Drm-NPF RIA [24] recognizes sNPFs. Aliquots (100–200 μl) of each HPLC fraction were lyophilized and then rehydrated with 220 μl RIA buffer (0.05 M Tris–HCl, pH 7.2; 0.1% bovine serum albumin; 0.02% sodium azide). Duplicate samples (100 μl) of each fraction were incubated overnight (4 °C) with Drm-NPF antiserum (403C; 1:25 K–1:50 K final dilution; bound/free ratio = 1 in the absence of unlabeled peptide) and ^{125}I-Drm-sNPF1D-Y^0 (10 K cpm). Bound and free ^{125}I-Drm-sNPF1D-Y^0 in sample tubes were separated by centrifugation after the addition of a mixture of activated charcoal–dextran–goat serum, and the pellets counted. For each RIA, a standard curve was plotted from the bound/free ratios and log values of synthetic Drm-sNPF2$_{9–19}$. The amount of immunoreactive peptide in the HPLC fractions of hemolymph and body extract was calculated from a regression equation for the linear portion (consistently 62.5 and 1000 fmol) of the sNPF2-$_{9–19}$ standard curve.

2.6. Membrane preparation

Membranes were prepared from Drm-NPFR76F cells using differential centrifugation through sucrose. Cells were grown to confluence in RPMI 1640 medium containing 800 μg/ml G418. The cells from 4 – 75 cm^2 flasks were washed two times in ice cold PBS, and then scraped from the flask after addition of 10 ml homogenization buffer (50 mM Tris–HCl, pH 7.5, 250 mM sucrose, with one protease inhibitor tablet/10 ml buffer (complete, mini; Roche). The plates were washed with 5 ml homogenization buffer to remove any additional cells. The scraped cells in homogenization buffer were put into a 50 ml Oak Ridge tube on ice and homogenized 4 × 30 s in a tissue mizer at maximum speed, and the homogenate centrifuged (2000 × *g*) for 10 min at 4 °C. The supernatant was transferred to a fresh tube on ice, and 6 ml of homogenization buffer added to the pellet and homogenized and spun as above. After the final spin, the supernatants were pooled and membranes collected by centrifugation at 48,000 × *g* for 1 h. The pelleted membranes were resuspended in 1 ml 50 mM Tris–HCl, pH 7.5 containing protease inhibitors, and the membranes were sheared through a 25-gauge needle, aliquotted and stored at −80°C until used.

2.7. Binding assays

Binding of ^{125}I-Drm-sNPF1D-Y^0 to membranes prepared from Drm-NPFR76F cells or from control cells transfected with plasmid alone was done as follows: membranes equivalent to 2 × 10^5 cells (that of a 24 well cell culture plate) were added to a 1.5 ml Eppendorf tube containing 100 pM ^{125}I-Drm-sNPF1D-Y^0 in 50 mM Tris–HCl, pH 7.5, 1× Hank's Balanced Salt solution, 1.5% BSA and protease inhibitor tablet (1 tablet/10 ml buffer) in the presence of various amounts of unlabeled peptide (0–1 μM). The binding reaction went for 2 h at room temperature vortexing every 30 min. To end the reaction, the tubes were centrifuged at 14,000 × *g* for 5 min at 4 °C, the supernatant aspirated and pellets washed three times with ice cold PBS. After the final wash, the bottoms of the microfuge tubes were cut off and counted on a Packard GammaII counter. Binding of ^{125}I-Drm-NPF and ^{125}I-PYY to whole cells was done as previously described [9]. The raw counts obtained from the binding assays were converted to percent total binding, and these data analyzed by non-linear regression analysis with GraphPad Prism software (v3.0 GraphPad Software Inc., San Diego, CA) to obtain curves, IC_{50} values (the concentration of sNPF that reduces specific binding of ^{125}I-Drm-sNPF1D-Y^0 by 50%) and statistics, including values of R^2 and standard errors.

3. Results

3.1. Identification of Drm-sNPFs in hemolymph and body extract

To determine which forms of Drm-sNPF are present in the fruitfly, hemolymph and whole body extract samples, fol-

lowed by synthetic peptide standards, were separately fractionated by HPLC to compare elution times, and immunoreactive fractions were detected with the Drm-NPF RIA. HPLC fractions from hemolymph sample and whole body extract were immunoreactive between 21 and 39 min (Fig. 1A and B), consistent with that of the peptide standards, which eluted between 19 and 39 min in the HPLC profile (Fig. 1C). Immunoreactive fractions from the initial HPLC separations of whole body or hemolymph samples were pooled, lyophilized, and purified further by a second HPLC purification as described in the materials and methods (data not shown). For hemolymph and body extract, immunoreactive fractions were pooled into three elution groups: (1) 16-20 min, (2) 20–25 min, and (3) 25–32 min. Each group was then fractionated a third time using the initial HPLC conditions. Immunoreactive fractions from the third round of HPLC fractionation were subjected to mass spectroscopy to determine identity. In the hemolymph, peptides with masses corresponding to Drm-sNPF1, Drm-sNPF2$_{9–19}$, and Drm-sNPF3 were found (Table 2). Additionally, a peptide with a mass corresponding to Drm-sNPF2$_{11–19}$ was also found (Table 2). In body extract samples, peptides with masses corresponding to Drm-sNPF1, Drm-sNPF1$_{4–11}$, Drm-sNPF3, and Drm-sNPF4 were found (Table 2). Additionally, peptides with masses corresponding to Drm-sNPF2$_{2–19}$, Drm-sNPF2$_{3–19}$, and Drm-sNPF2$_{11–19}$ were also found in body extract samples (Table 2).

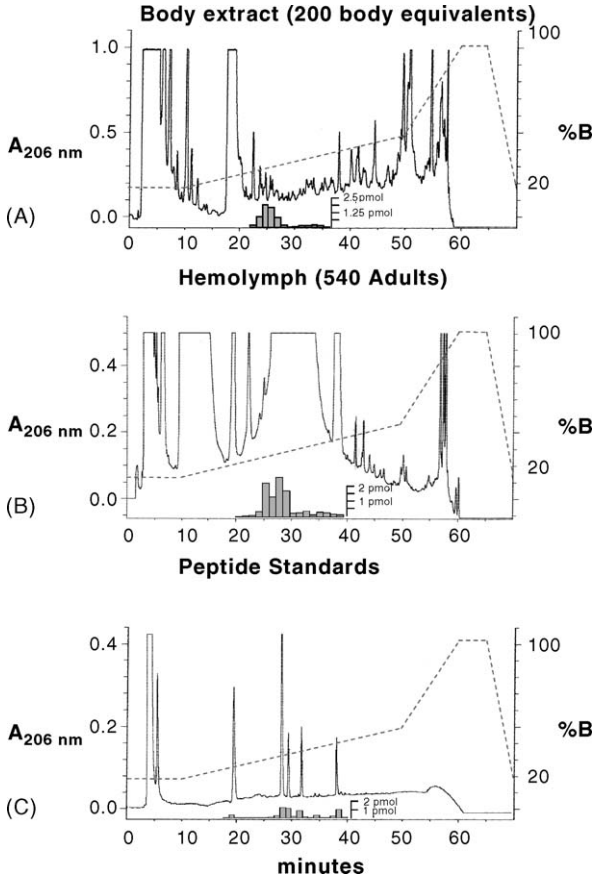

Fig. 1 – HPLC elution of Drm-sNPFs in (A) acetic acid whole body extract of adult *D. melanogaster* males and females, (B) hemolymph pooled from adult *Drosophila melanogaster* males and females, and (C) synthetic reference peptides. For the latter, corresponding elution times were: Drm-sNPF4, 19 min; Drm-sNPF3, 28 min; Drm-sNPF1$_{4–11}$, 28 min; Drm-sNPF1, 29 min; Drm-sNPF2$_{9–19}$, 31 min; and Drm-sNPF2; 38 min. Hemolymph, acetic acid extract and synthetic peptides were fractionated separately on a C_{18} column with a gradient of solvent B (0.1%TFA in 80% CH_3CN; 20–50% B, 40 min, 50–100% B, 10 min; 1 ml/min; monitored at 206 nm). Drm-sNPF-containing fractions were determined by an RIA using an antibody for Drm-NPF (403C).

3.2. *Analysis of Drm-sNPF, Ang-sNPF and AeaHP binding to Drm-NPFR76F*

To assess the relative affinities of Drm-sNPFs to Drm-NPFR76F a radioreceptor approach was taken. Membranes of Drm-NPFR76F cells specifically bound ^{125}I-Drm-sNPF1D-Y^0, and this binding was displaced by the addition of Drm-sNPF1 in a concentration-dependent manner (Fig. 2). An IC_{50} of ~0.3 nM was calculated from the Drm-sNPF1 binding data (Table 1). Each Drm-sNPF displaced ^{125}I-Drm-sNPF1D-Y^0 in a concentration-dependent manner (Fig. 2). The rank order of potency was Drm-sNPF1 ~ Drm-sNPF2$_{9–19}$ ~ Drm-sNPF2 ~ Drm-sNPF2$_{11–19}$ > Drm-sNPF4 ~ Drm-sNPF1$_{4–11}$ > Drm-sNPF3 (Table 1). Similarly, Drm-sNPF1D-Y^0 competed ^{125}I-Drm-sNPF1D-Y^0 binding effectively (data not shown). In contrast, membranes from control cells exhibited no specific binding for ^{125}I-Drm-sNPF1D-Y^0 (data not shown). In addition, neither ^{125}I-Drm-NPF nor ^{125}I-PYY bound specifically to Drm-NPFR76F cells (data not shown).

Related peptides from the mosquitoes *A. gambiae* and *A. aegypti* were also tested for their ability to displace ^{125}I-Drm-sNPF1D-Y^0 binding to the *Drosophila* sNPF receptor. There are five potential Ang-sNPFs encoded in the *A. gambiae* genome, three with a C-terminal LRLRFa motif and two with an RLRWa C-terminus (Table 1). Each displaced ^{125}I-Drm-sNPF1D-Y^0 bound to membranes prepared from Drm-NPFR76F cells in a concentration dependent manner (Fig. 3A). The rank order of potency was Ang-sNPF1 > Ang-sNPF2 ~ Ang-sNPF4 ~

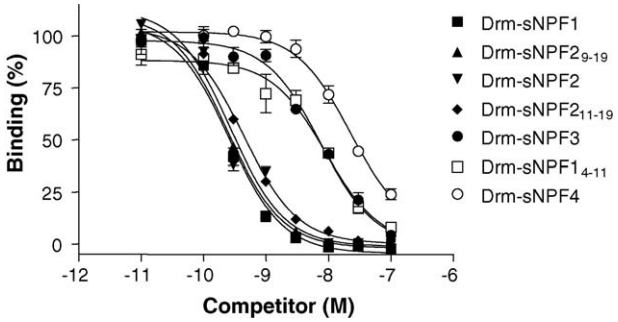

Fig. 2 – Competitive inhibition of ^{125}I-Drm-sNPF1D-Y^0 binding to membranes prepared from CHO-K1 cells stably transfected with Drm-NPFR76F cDNA by Drm-sNPFs. Membranes were incubated with 100 pM ^{125}I-Drm-sNPF1D-Y^0 and various concentrations of Drm-sNPF1, Drm-sNPF2$_{11–19}$, Drm-sNPF1$_{4–11}$, Drm-sNPF2, Drm-sNPF2$_{9–19}$, Drm-sNPF3, or Drm-sNPF4 for 3 h at room temperature. Values indicate mean ± S.E. (N = 3).

Table 2 – Drm-sNPF peptides detected in adult hemolymph and body extract

Peptide	Sequence	Predicted mass	Observed mass	Hemolymph	Body
sNPF1	AQRSPSLRLRFa	1329,1351(Na), 1367(K)	1330	+[a]	+
$sNPF1_{4–11}$	SPSLRLRFa	974,996(Na), 1012(K)	974	ND[b]	+
$sNPF2_{2–19}$	FGDVNQKPIRSPSLRLRFa	2129,2151(Na), 2167(K)	2129, 2150	ND	+
$sNPF2_{3–19}$	GDVNQKPIRSPSLRLRFa	1982,2004(Na), 2022(K)	2023	ND	+
$sNPF2_{9–19}$	PIRSPSLRLRFa	1340,1362(Na), 1378(K)	1362	+	ND
$sNPF2_{11–19}$	RSPSLRLRFa	1130,1152(Na), 1168(K)	1132, 1154	+	+
sNPF3	PMRLRWa	857,879(Na), 895(K)	879, 895	+	+
sNPF4	PQRLRWa	854,876(Na), 892(K)	877	ND	+

[a] (+) Detected.
[b] ND: not detected.

Aea-sNPF2 > Ang-$sNPF1_{4–11}$ ~ Ang-$sNPF2_{4–11}$ ~ Ang-sNPF3 ~ Ang-sNPF5 (Table 1). The *Aedes* head peptides, having a C-terminal LKTRFa motif, were also tested for their ability to displace ^{125}I-Drm-sNPF1D-Y^0 binding to the *Drosophila* sNPF receptor. Only Aea-HPI was able to displace ^{125}I-Drm-sNPF1D-Y^0 bound to membranes prepared from Drm-NPFR76F cells in a concentration dependent manner (Fig. 3B), with an IC_{50} of 42.4 nM (Table 1); in contrast, Aea-HPIII (1 μM) was unable to displace ^{125}I-Drm-sNPF1D-Y^0 (Fig. 3B).

The C-terminal amino acid sequence of sNPFs is important for peptide interaction with Drm-NPFR76F [16]. The apparent high-affinity binding of sNPFs tested in this study fell into two groups, those with IC_{50} values in the nanomolar range, and those with IC_{50} values in the sub-nanomolar range. The latter group was composed of longer sNPFs (≥9 amino acids); notably, each of these possessed an arginine residue in the ninth position from the C-terminus, with Drm-$sNPF2_{11–19}$ representing the minimal size. Removal of this residue, as in Drm-$sNPF1_{4–11}$, markedly reduced apparent affinity. Accordingly, an alanine replacement analog, Drm-$sNPF2_{11–19}$R11A, was tested. This analog displaced ^{125}I-Drm-sNPF1D-Y^0 from Drm-NPFR76F cells in a concentration dependent manner (Fig. 4), but resembled Drm-$sNPF1_{4–11}$ in activity. The rank order of potency was Drm-sNPF1 ~ Drm-$sNPF2_{11–19}$ > Drm-$sNPF2_{11–19}$R11A ~ Drm-$sNPF1_{4–11}$ (Table 1, Fig. 4).

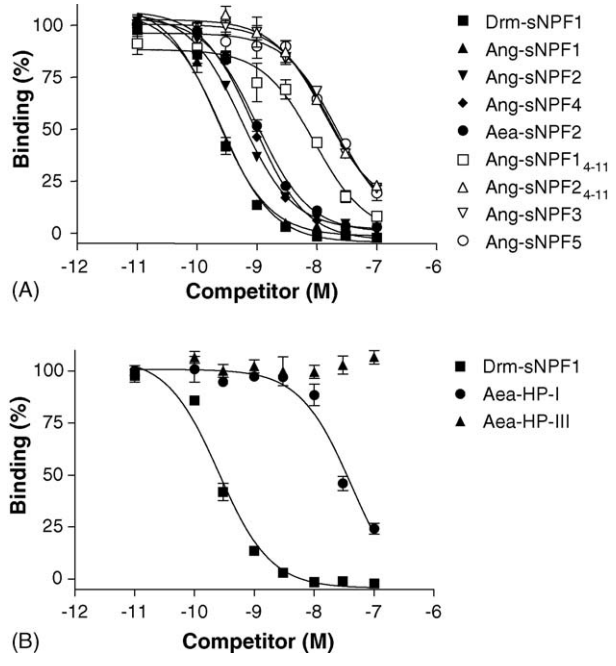

Fig. 3 – Competitive inhibition of ^{125}I-Drm-sNPF1D-Y^0 binding to membranes prepared from Drm-NPFR76F cells by Ang-sNPFs and Aea-HPs. Membranes were incubated with 100 pM ^{125}I-Drm-sNPF1D-Y^0 and various concentrations of (A) Drm-sNPF1, Ang-sNPF1, Ang-$sNPF1_{4–11}$, Ang-sNPF2, Ang-$sNPF2_{4–11}$, Ang-sNPF3, Ang-sNPF4, Ang-sNPF5, or Aea-sNPF2; (B) Drm-sNPF1, Aea-HPI or Aea-HPIII for 3 h at room temperature. Values indicate mean ± S.E. (N = 3).

4. Discussion

Detailed understanding of the actions of sNPFs requires a greater knowledge both of their structures and of their signaling mechanisms. For *D. melanogaster*, the identification of individual sNPF peptide sequences has been somewhat elusive, despite an evident gene. Similarly, activity studies of candidate sNPFs in relation to activation of the apparent sNPF receptor have yielded mixed results. The present investigation was undertaken to clarify further the occurrence of sNPF peptides and to examine directly structural features of receptor binding by radioreceptor assay.

Following the elaboration of the *D. melanogaster* genome, Vanden Broeck [25] took an *in silico* approach to identify a gene encoding the sNPF precursor, which was suggested to contain four distinctive sNPF peptides. The likelihood that the precursor encoded four sNPFs was indicated by the presence both of flanking di-basic amino acid cleavage sites and of signature motifs for C-terminal amidation. However, the sequences of the resulting peptides are not unambiguous, due to additional arginine residues that may act as internal cleavage sites. The straightforward nomenclature for sNPF1-4 as proposed by Vanden Broeck [25] has been adopted in the present report.

Information about the specific sequences of putative peptides produced from the sNPF precursor has been accumulating slowly. Proteomic approaches have provided structural evidence supporting the existence of sNPF1 and sNPF2 in *D. melanogaster*. Baggerman et al. [1,2] employed tandem mass spectrometry to identify peptide sequences in extracts of pooled CNS of wandering larvae. A mass corresponding to the peptide sequence SPSLRLRFa was identified, which these authors attributed as sNPF1 (herein designated $sNPF1_{4–11}$). Also found was a mass corresponding

to the first 10 amino acids (WFGDVNQKPI; $sNPF2_{1–10}$) of sNPF2, implying that the full-length, 19 residue sNPF2 may occur as a precursor product in vivo. Identification of an additional internal (non-sNPF) sequence in these analyses by mass spectrometry also validates the view that the sNPF precursor is processed into at least some of the products predicted. With the possibility of tryptophan loss concurrent with acid extraction, the inference that sNPF2 in particular is a product is supported by the detection of a mass corresponding to $sNPF2_{2–19}$ (see below) in the present study.

An elegant mass spectrometric analysis of individual nerve tissues and abdominal neurohemal organs [19] extended the identification of sNPF precursor products to adult *D. melanogaster*. In the neurohemal complex of the corpora cardiaca and hypocerebral ganglion, masses were found corresponding to sNPF1, $sNPF1_{4–11}$, and $sNPF2_{1–10}$, confirming that both the sNPF1 and sNPF2 sequences likely are derived from the parent precursor in vivo. For peptidergic neurons supplying neurohemal sites, examination of pars intercerebralis cells from the brain also revealed $sNPF1_{4–11}$. Particularly intriguing was the detection of sNPF1 both in the posterior corpora cardiaca/hypocerebral ganglion complex and in the aorta directly behind. Finding of sNPFs at such neurohemal release sites indicates a likely neurosecretory role.

To determine structures of sNPFs, the present investigation utilized adult *D. melanogaster* of mixed sex and focused on acidic extracts both of body and of hemolymph. An RIA for sNPF was used to guide partial purification of extracts by HPLC prior to analysis by mass spectrometry; only immunoreactive peptides containing the C-terminal sNPF sequence were detected due to the assay specificity. The resultant purified materials indicated the presence of sequences of a full spectrum of sNPF peptides. Bodies contained sNPF1, $sNPF1_{4–11}$, sNPF3, and sNPF4; sNPF2 was evident in several truncated forms ($sNPF2_{2–19}$, $sNPF2_{3–19}$, $sNPF2_{11–19}$; see Table 1). Hemolymph exhibited sNPF1, $sNPF2_{9–19}$, $sNPF2_{11–19}$, and sNPF3, further suggesting a possible neuroendocrine role. Body and hemolymph both exhibited RSPSLRLRFa (see also discussion above), the origin of which is somewhat ambiguous, because this sequence appears in both sNPF1 and sNPF2. Because of the reported occurrence of $sNPF2_{1–10}$ [1,2,19], a fragment corresponding exactly to the remaining N-terminal portion of sNPF2, we consider it likely that RSPSLRLRFa is a product of sNPF2 and designate it as $sNPF2_{11–19}$.

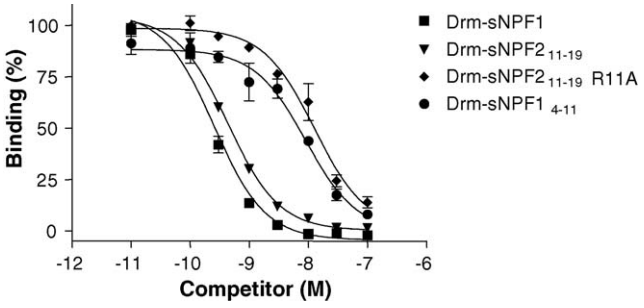

Fig. 4 – Competitive inhibition of ^{125}I-Drm-sNPF1D-Y^0 binding to membranes prepared from Drm-NPFR76F cells by selected Drm-sNPFs and an analog. Membranes were incubated with 100 pM ^{125}I-Drm-sNPF1D-Y^0 and various concentrations of Drm-sNPF1, Drm-$sNPF1_{4–11}$, Drm-$sNPF2_{11–19}$, or Drm-$sNPF2_{11–19}$R11A for 3 h at room temperature. Values indicate mean ± S.E. (N = 3).

The sNPFs of *D. melanogaster* differ in their interactions with the sNPF receptor Drm-NPFR76F, as analyzed directly by radioreceptor assay. A wide variety of *D. melanogaster* sNPFs were assayed for their ability to inhibit the binding of ^{125}I-[D-Y^1]-Drm-sNPF1 to membranes prepared from cells stably transfected with Drm-NPFR76F. Two distinctive classes of activity of sNPFs were readily apparent. The sNPF peptides containing nine or more amino acids typically exhibited high affinity, as judged by an $IC_{50} < 1$ nM, whereas peptides containing eight for fewer amino acids exhibited IC_{50} values of >5 nM. Those exhibiting lower affinity included sNPF3 and sNPF4, peptides with the C-terminal RLRWa sequence. The minimum length of the highly active group was represented by $sNPF2_{11–19}$. The sequence of this $sNPF2_{11–19}$ (RSPSLRLRFa) differs from $sNPF1_{4–11}$ (SPSLRLRFa) only by a single arginine residue, which appears to confer a substantial increase in binding affinity. To test this hypothesis, an alanine substituted analog, Drm-$sNPF2_{11–19}$R11A, was assayed and found to exhibit a substantial drop in activity, with an IC_{50} of only 12.5 nM, indicating the crucial role of this arginine residue.

For further tests of these apparent structure-function relations, putative sNPFs identified in the genomes of *A. gambiae* [21] and *A. aegypti* ([21] and present study) also were examined in the Drm-NPFR76F radioreceptor assay. Each of these mosquito sNPF peptides conformed to the distinctive pattern of length-associated activity established previously for those of *D. melanogaster*. In contrast, the *A. aegypti* head peptides [14] which partly resemble sNPFs [10] were either weakly active, Aea-HP-I, or inactive, Aea-HP-III, despite being of sufficient length and having the requisite arginine (see above). Accordingly, additional structural features in the C-terminus common to sNPF peptides appear important for high affinity binding.

Identifications of candidate ligands for orphan G-protein-coupled receptors have relied on a variety of approaches [15], typically involving receptor expression in heterologous cells. For *D. melanogaster*, previous studies consistently specify Drm-NPFR76F as the cognate sNPF receptor [8,16,20]. However, each study, including the present investigation, exhibits some differences relative to the activities of various sNPFs tested. In the aggregate, a clear focus on the structure-function relations between sNPFs and this receptor remains somewhat elusive, perhaps reflective of cell expression and methodological differences.

One informative approach has involved using a bioluminescent calcium response as an indicator of receptor activation for CHO-K1 cells transfected with Drm-NPFR76F [16]. In this assay, the *D. melanogaster* sNPFs (sNPF1, $sNPF1_{4–11}$, sNPF3, sNPF4) tested were found to be roughly equipotent, based on comparable EC_{50} values (31–75 nM) derived from dose–response curves. The structurally related *Schistocerca gregaria* sNPF (*Scg*-NPF, YSQVARPRFa; EC_{50} = 120 nM) also was somewhat active, but peptides other than sNPFs (e.g. *Scg*-FLRFa) were ineffective at the doses tested. For values of maximal bioluminescent response (Fig. 5 in [16]), sNPF peptide length appeared to correlate with activity. The longer sNPF1 elicited the highest maximum, with the short sNPF3 and sNPF4 the

least, and sNPF1$_{4-11}$ intermediate; the maximal response may be related to efficacy of receptor activation.

Another assay based on coexpression of Drm-NPFR76F with the promiscuous G-protein $G_{\alpha 16}$ in *Xenopus* oocytes [8,20] was used to evaluate the activity of a panel of *D. melanogaster* sNPFs. Receptor activation was measured by induction of either inwardly directed chloride currents [8] or inwardly directed potassium currents [20]. The pattern of responses for *D. melanogaster* sNPFs was similar by either measurement. Longer sNPF peptides (sNPF1, sNPF2, sNPF2$_{11-19}$) were both more potent, as determined by EC_{50}, and more effective, at a test dose of 1 μM, than were shorter sNPFs (sNPF1$_{4-11}$, sNPF3, sNPF4). In this assay system, *Led*-sNPF1 and *Led*-sNPF2 were in many respects found comparable to the longer *D. melanogaster* sNPFs; assorted other peptides tested exhibited relatively nominal activity, more comparable to the shorter *D. melanogaster* sNPFs.

For the *D. melanogaster* sNPF receptor, comparisons of activities among assay systems based on disparate approaches require caution in interpretation. The approach of estimating apparent binding affinities by radioreceptor assay is intrinsically limited by the expression of an insect peptide receptor in vertebrate cells. Similar limitations apply to assays measuring activation of heterologously expressed receptors [8,16,20]. Nonetheless, for *D. melanogaster* sNPF peptides, longer (≤9 amino acids) forms appear more active than shorter (≤8 amino acids) ones, when the data from all receptor assays are considered in the aggregate.

For *D. melanogaster*, a physiological role for sNPFs in the regulation of feeding behavior of larvae and adults has been recently reported [13]. Food intake was stimulated in gain-of-function *sNPF* mutants, with overexpression resulting in larger flies. In contrast, loss-of-function *sNPF* mutants exhibited reduced food intake. Northern and Western blot analyses revealed sNPF transcripts and peptides in all developmental stages. In situ hybridization (embryos and larvae) and immunohistochemistry (embryos, larvae, and adults) localized sNPF widely within nervous tissues, but not in gut; the observation of sNPF immunostaining in dorsal neurohemal organs above the fused thoracic ganglia supports a potential neurosecretory role (see also above).

The Drm-NPFR76F receptor clearly is also localized in the nervous system and may occur in other tissues as well. In the embryo, in situ hybridization demonstrates the presence of receptor transcripts in the nervous system [8]. Northern blot analyses of adults also suggest the receptor occurs abundantly in heads, moderately in legs and appendages, and only slightly in body [8]. In contrast, a widespread distribution of the receptor was indicated by RT-PCR with cDNA from brain, gut, fat body, and Malpighian tubules of larvae and for heads, bodies, and ovaries of adults [16]. Although the reasons for these disparate observations are not readily apparent, detection of receptors occurring with differing abundance may vary according to the method employed.

Drm-NPFR76F belongs to a structurally related group of invertebrate receptors that resemble mammalian type 2 neuropeptide Y receptors (see [8,10]). Like their vertebrate counterparts, these invertebrate receptors have been implicated in regulation of feeding and related digestive processes ([13,22,26,27]; see also [7]). In larval *A. aegypti*, Aea-sNPF2$_{4-11}$ has been shown to inhibit peristalsis of the anterior stomach in vitro [18], an action that could effect both digestion and feeding in vivo.

In *C. elegans*, members of this receptor family participate in regulation of both feeding and reproduction (see [11]). One that resembles Drm-NPFR76F [17] modifies egg laying in *C. elegans*, as shown by RNAi experiments [12]. Intriguingly, the first activity ascribed to sNPF was the stimulation of ovarian development [4,6] in adult migratory locusts, *Locusta migratoria*, following injections with *Led*-sNPF1. Of note, the longer *Led*-sNPF1 was found to be ten-fold more potent biologically than the shorter *Led*-sNPF2 [4], consistent with the pattern of structural activity found for binding of *D. melanogaster* sNPFs to Drm-NPFR76F in the present study. Much remains to be understood about the mode of action of sNPFs and their receptors. Their apparent participation in the physiologically interrelated processes of reproduction and of feeding and digestion suggests the importance of such future studies.

Acknowledgments

We thank Dr. Kevin Clark for syntheses of sNPF peptides and Mr. Cory Lee for assistance with cell culture. This work was supported by grants to M.R.B. from the Georgia Experiment Station (GEO00786) and National Institutes of Health (AI33108).

REFERENCES

[1] Baggerman G, Boonen K, Verleyen P, De Loof A, Schoofs L. Peptidomic analysis of the larval *Drosophila melanogaster* central nervous system by two-dimensional capillary liquid chromatography quadrupole time-of-flight mass spectrometry. J Mass Spectrom 2005;40(2):250–60.
[2] Baggerman G, Cerstiaens A, De Loof A, Schoofs L. Peptidomics of the larval *Drosophila melanogaster* central nervous system. J Biol Chem 2002;277(43):40368–74.
[3] Brown MR, Crim JW, Arata RC, Cai HN, Chun C, Shen P. Identification of a *Drosophila* brain-gut peptide related to the neuropeptide Y family. Peptides 1999;20(9): 1035–42.
[4] Cerstiaens A, Benfekih L, Zouiten H, Verhaert P, De Loof A, Schoofs L. Led-NPF-1 stimulates ovarian development in locusts. Peptides 1999;20(1):39–44.
[5] Crim JW, Garczynski SF, Brown MR. Approaches to radioiodination of insect neuropeptides. Peptides 2002;23(11):2045–51.
[6] De Loof A, Baggerman G, Breuer M, Claeys I, Cerstiaens A, Clynen E, et al. Gonadotropins in insects: an overview. Arch Insect Biochem Physiol 2001;47(3):129–38.
[7] Dockray GJ. The expanding family of -RFamide peptides and their effects on feeding behaviour. Exp Physiol 2004;89(3):229–35.
[8] Feng G, Reale V, Chatwin H, Kennedy K, Venard R, Ericsson C, et al. Functional characterization of a neuropeptide F-like receptor from *Drosophila melanogaster*. Eur J Neurosci 2003;18(2):227–38.
[9] Garczynski SF, Brown MR, Shen P, Murray TF, Crim JW. Characterization of a functional neuropeptide F receptor from *Drosophila melanogaster*. Peptides 2002;23(4): 773–80.

[10] Garczynski SF, Crim JW, Brown MR. Characterization of neuropeptide F and its receptor from the African malaria mosquito, *Anopheles gambiae*. Peptides 2005;26(1):99–107.
[11] Geary TG, Kubiak TM. Neuropeptide G-protein-coupled receptors, their cognate ligands and behavior in Caenorhabditis elegans. Trends Pharmacol Sci 2005;26(2):56–8.
[12] Keating CG, Kriek N, Daniels M, Ashcroft NR, Hopper NA, Siney EJ, et al. Whole-genome analysis of 60 G protein-coupled receptors in Caenorhabditis elegans by gene knockout with RNAi. Curr Biol 2003;13(19):1715–20.
[13] Lee KS, You KH, Choo JK, Han YM, Yu K. *Drosophila* short neuropeptide F regulates food intake and body size. J Biol Chem 2004;49(3):50781–9.
[14] Matsumoto S, Brown MR, Crim JW, Vigna SR, Lea AO. Isolation and primary structure of neuropeptides from the mosquito, *Aedes aegypti*, immunoreactive to FMRFamide antiserum. Insect Biochem 1989;19:277–83.
[15] Meeusen T, Mertens I, De Loof A, Schoofs L. G protein-coupled receptors in invertebrates: a state of the art. Internat Rev Cytol 2003;230:189–261.
[16] Mertens I, Meeusen T, Huybrechts R, De Loof A, Schoofs L. Characterization of the short neuropeptide F receptor from *Drosophila melanogaster*. Biochem Biophys Res Commun 2002;297(5):1140–8.
[17] Mertens I, Vandingenen A, Meeusen T, Janssen T, Luyten W, Nachman RJ, et al. Functional characterization of the putative orphan neuropeptide G-protein coupled receptor C26F1.6 in Caenorhabditis elegans. FEBS Lett 2004; 573(1–3):55–60.
[18] Onken H, Moffett SB, Moffett DF. The anterior stomach of larval mosquitoes (*Aedes aegypti*): effects of neuropeptides on transepithelial ion transport and muscular motility. J Exp Biol 2004;207(21):3731–9.
[19] Predel R, Wegener C, Russell WK, Tichy SE, Russell DH, Nachman RJ. Peptidomics of CNS-associated neurhemal systems of adult *Drosophila melanogaster*: a mass spectrometric survey of peptides from individual flies. J Comp Neurol 2004;474(3):379–92.
[20] Reale V, Chatwin HM, Evans PD. The activation of G-protein gated inwardly rectifying K+ channels by a cloned *Drosophila melanogaster* neuropeptide F-like receptor. Eur J Neurosci 2004;19(3):570–6.
[21] Riehle MA, Garczynski SF, Crim JW, Hill CA, Brown MR. Neuropeptides and peptide hormones in *Anopheles gambiae*. Science 2002;298(5591):172–5.
[22] Shen P, Cai HN. *Drosophila* neuropeptide F mediates integration of chemosensory stimulation and conditioning of the nervous system by food. J Neurobiol 2001;47(1):16–25.
[23] Spittaels K, Verhaert P, Shaw C, Johnston RN, Devreese B, Van Beeumen J, et al. Insect neuropeptide F (NPF)-related peptides: isolation from Colorado potato beetle (*Leptinotarsa decemlineata*) brain. Insect Biochem Mol Biol 1996;26(4): 375–82.
[24] Stanek DM, Pohl J, Crim JW, Brown MR. Neuropeptide F and its expression in the yellow fever mosquito *Aedes aegypti*. Peptides 2002;23(8):1367–78.
[25] Vanden Broeck J. Neuropeptides and their precursors in the fruitfly, *Drosophila melanogaster*. Peptides 2001;22(2):241–54.
[26] Wen T, Parrish CA, Xu D, Shen P. *Drosophila* neuropeptide F and its receptor, NPFR1, define a signaling pathway that acutely modulates alcohol sensitivity. Proc Natl Acad Sci USA 2005;102(6):2141–6.
[27] Wu Q, Wen T, Lee G, Park JH, Cai HN, Shen P. Developmental control of foraging and social behavior by the *Drosophila* neuropeptide Y-like system. Neuron 2003;39(1):147–61.